Zeitschrift: Schweizerische mineralogische und petrographische Mitteilungen = Bulletin suisse de minéralogie et pétrographie

Band: 69 (1989)

Heft: 1

Artikel: A hydrothermal manganiferous sulfide assemblage in Carbonif-erous volcanic rocks of the central Aar massif (Switzerland)

Autor: Abrecht, Jürgen

DOI: https://doi.org/10.5169/seals-52781

SCHWEIZ. MINERAL. PETROGR. MITT. 69, 117–128, 1989

A hydrothermal manganiferous sulfide assemblage in Carboniferous volcanic rocks of the central Aar massif (Switzerland)

by *Jürgen Abrecht*[1]

Abstract

A manganiferous sulfide-silicate-carbonate assemblage occurs in veins within a volcano-sedimentary sequence in the Variscan basement of the Aar massif in the Reuss Valley. The main constituent phases are alabandite (MnS), pyrrhotite, rhodonite, spessartine-grossular garnet, Mn-bearing amphiboles, and Mn calcite. An epithermal formation from hydrothermal solutions is assumed from geologic and mineralogical reasons. Later infiltration of water-rich fluids at low to moderate temperatures caused the oxidation/desulfidation of the primary sulfide ore. Phases formed during this first stage of alteration were calcic rhodonite, Mn-rich garnet, and Mn-calcite. In a second stage at greenschist-facies conditions, probably during the Alpine orogeny, Mn-rich amphiboles were formed mainly by hydration of the rhodonite. Along the vein-host rock contact grossular-rich garnet formed together with Mn-poor actinolites. The present phase assemblage still displays a mineralogical and chemical zoning, also reflected by the negative correlation between Ca and Mn in rhodonite, garnet and amphiboles from core to rim of the vein. The sulfide-rhodonite-Mn calcite assemblage indicates water-rich fluids with fs_2 below 10^{-3} and fo_2 below 10^{-28}.

Keywords: Sulfides, Mn-minerals, fluid, metamorphism, volcanic rocks, Variscan, Aarmassif, Switzerland.

Introduction

The occurrence of alabandite (MnS, alab) and Mn-silicates in a water tunnel of the Amsteg power plant of the Swiss Federal Railways was first described by HUGI (1921a). He reported "quartz-calcite pegmatites" with alabandite and rhodonite (rdn) and garnet as main constituents. At three different localities in the tunnel such veins crosscut chlorite-biotite schists that lie to the North of the Aar granite in the central Aar massif.

HUGI (1923) and HUTTENLOCHER (1936) reported the occurrence of Ag-Sn sulfide- and pyrrhotite-chalcopyrite veins (±PbS, ±ZnS) in the same host rock sequence. Both authors related the origin of the Mn-rich rocks to the intrusion of the Variscan Aar granite (290 Ma; SCHALTEGGER, 1986) and its postmagmatic hydrothermal activity. The Mn-silicates were interpreted by HUTTENLOCHER (1936) as product of the Tertiary metamorphic overprint. JENNY (1973) reported the occurrence of small, rounded grains of pyrrhotite (pyrrh) within the alabandite masses. He suggested an exsolution of a primary homogeneous Fe-Mn sulfide due to recrystallization during the Alpine orogeny.

Alabandite is not a very common phase in Mn deposits and is usually of hydrothermal origin (ROY, 1981). It is stable only under very reducing conditions at high sulfur fugacities (GARRELS and CHRIST, 1965). FUKUOKA (1981) reported its occurrence in a large number of vein-type deposits, but also in sedimentary deposits and claimed it to be stable under a rather wide range of P-T-X conditions. New data on the phase relations, the mineral composition, and textures as well as a physico-chemical and geological evaluation of the formation the Amsteg deposit will be presented in this study. The investigation was carried out on samples collected during the tunnel construction, now deposited in the Mineralogical Institute of the University of Berne.

Geologic situation and origin of the host rock

The Mn-rich rocks were collected in the tunnel at about 5.3 km N of Pfaffensprung or 310 m N from

[1] Mineralogisch-Petrographisches Institut Universität Basel, Bernoullistrasse 30, CH-4056 Basel. Present address: Mineralogisch-Petrographisches Institut Universität Bern, Baltzerstrasse 1, CH-3012 Bern, Switzerland.

the window V (Fig. 1a), which is less than 2 km from the Aar granite intrusion (to the S). Few details are known about the local host rocks. Based upon original notes and sketches and later publications by HUGI (1921a, 1921b, 1923), the following rock sequence along the tunnel profile can be given (from S to N):

– Aar granite	0-3456 m from Pfaffensprung
– banded biotite-gneisses, locally migmatitic	3456 - ca. 4900 m
– biotite gneisses with abundant mafic and ultramafic rocks, "quartz-porphyry dikes"	≈ 4900 - 5215 m
– chlorite-biotite-schists with "quartz-porphyry dikes"	5215 - 5340 m
– chlorite-biotite-schists and -gneisses, often quartz-rich (HUGI: "hornfelses"),	5340-ca. 5500 m
– biotite-chlorite-schists and -gneisses, sericite-chlorite-schists with Carboniferous shales and coals	5500 - 5640 m

These rocks are followed by the pre-Variscan Erstfeld gneiss zone to the N of the Maderaner Valley. According to HUGI (1923) and HUTTENLOCHER (1936) the whole rock series to the N of the Aar granite comprises part of the Variscan basement. This basement was intruded during the Carboniferous by the Aar granite magma and its subvolcanic successors ("quartz-porphyry dikes"), some of which occasionally crosscut the granite.

PFLUGSHAUPT's (1927) map includes a "quartz-porphyry" zone containing Carboniferous sediments. On his map, this zone is accompanied on either side by sericite-schists and -gneisses of unclear origin.

In contrast, SCHENKER (1986, 1987) considers the sericite-schists and biotite-sericite gneisses to be a volcano-sedimentary rock sequence. This sequence, together with the "quartz-porphyry dikes", makes up part of the "Lötschen-Färnigen zone" which consists of Paleozoic and Mesozoic rocks. As a whole, the volcano-sedimentary series in the Reuss Valley and the volcano-sedimentary rock sequences from the "Tscharren"-Formation and the "Windgällen"-Formation form the Maderaner-Group (OBERHÄNSLI et al., 1988; SCHENKER, 1986, 1987). Thus, these rocks are of Upper-Paleozoic age, but have suffered late-Paleozoic deformation before they were intruded by the Aar granite (see also SCHENKER and ABRECHT, 1987). The "quartz-porphyry dikes" of the earlier authors are interpreted by SCHENKER (1986) as members of ignimbritic flow sequences rather than as intrusive dikes.

The rocks display greenschist-facies mineral assemblages (JENNY, 1973), but some mineral as-

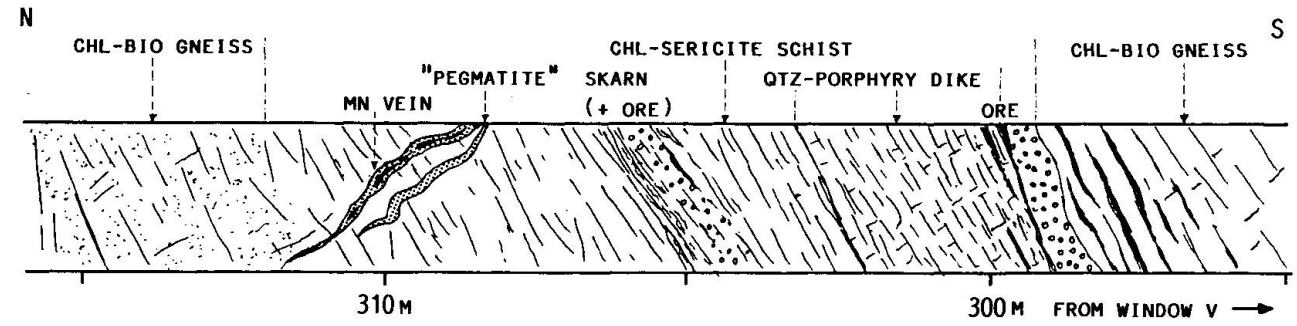

Fig. 1a Geologic section in Amsteg water tunnel between 295 and 315 m N from window V (2255 to 2275 metres from Pfaffensprung. Redrawn from original sketches with rock names given by the author (HUGI, 1921b). Note the discordant character of the Mn veins. The rocks in this section represent a silicic tuffaceous series (gneisses) with an intercalated ignimbritic flow ("qtz-porphyry dike"). Ores are: FeS_2, Fe_2O_3, $FeCuS_2$, PbS and ZnS.

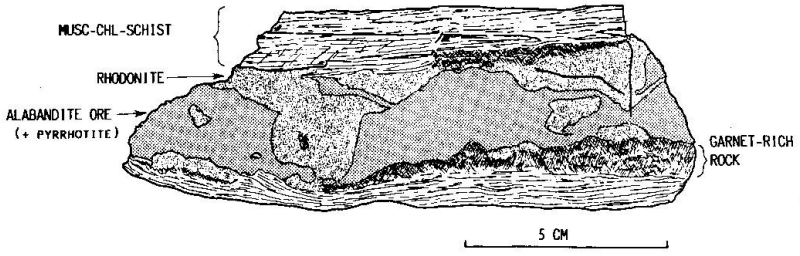

Fig. 1b Sketch of sulfide-rich vein. The sulfide core (alabandite + pyrrhotite) is replaced by silicates and carbonate. Garnet preferentially occurs along the contact with the gneiss.

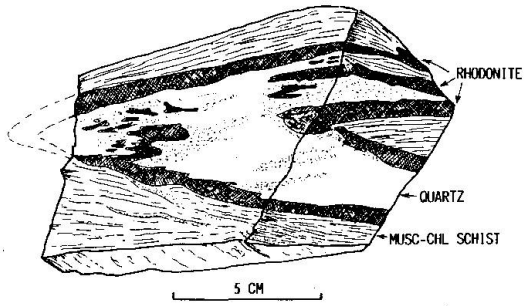

Fig. 1c Folded sulfide-free rhodonite-quartz vein (±carbonate, ±garnet, ±amphibole). Probably from the vein labelled "pegmatite" in Fig. 1a.

semblages may reflect their primary volcanic origin, altered by hydrothermal activities (see below). Temperatures and pressures reached during the Tertiary metamorphism were 350 to 400°C and about 3 kbars (FREY et al., 1980). The basement rocks which are cut by the Aar granite (290 Ma, SCHALTEGGER , 1986) have suffered an earlier (pre-Variscan) amphibolite-facies metamorphism (SCHENKER, 1986; SCHENKER and ABRECHT, 1987).

Sulfide occurrences are mostly restricted to the chlorite-biotite schists with its numerous ignimbritic intercalations ("quartz-porphyries"). These occurrences were subdivided by HUTTENLOCHER (1936) into three groups:

(a) ores with $CuFeS_2$, FeS, FeS_2, ZnS, PbS; always with Sn- and Ag-sulfides (e.g. at 5260 metres)

(b) FeS-$CuFeS_2$ ores, but without PbS, ZnS and the Sn-Ag-sulfides; are generally related to mafic-ultramafic rocks

(c) MnS-FeS, with manganiferous silicates (at 5270, 5372, 5450 metres). The Fe-Cu-Pb-Zn-sulfide deposits occurring on the surface in this area were later described in detail by JENNY (1973).

JENNY (1973) already pointed out the non-pegmatitic character of the Mn ore. Indeed, the available samples rather suggest a vein-type sulfide deposit. Two Mn-rich vein types can be distinguished:

a) a sulfide-rich assemblage displaying a zonation (Mn vein in Fig. 1a, Fig. 1b) and b) a quartz-rich sulfide-free rhodonite-carbonate±garnet rock (Fig. 1c). In fact, the latter has a pegmatitic appearance and was described by HUGI (1921b) as pegmatite (given as "pegmatite" in Fig. 1a), but most likely represents a more altered stage of an originally sulfide-rich vein (see below).

Mineralogy of the vein and adjoining host rock

THE HOST ROCK

Unfortunately the available samples include only limited portions of the host rock and so cannot yield representative petrological and mineralogical data. However, some observations can be made that bear upon the exchange of elements between vein and host rock: Alkali feldspars are replaced to varying extent by muscovite (sericite), usually along the borders. Plagioclase is not present and seems to be only a minor constituent in this zone (PFLUGSHAUPT, 1927). While fresh brown biotites have low MnO-contents (< 1 wt%), partially chloritized grains have increased contents (> 1 wt%), and chlorites grown at the expense of biotites have MnO-contents in the range 1.5 to 2 wt% (Table 1). Garnets grown within the altered gneiss along the Mn-vein have a high spessartine component (40-50 mol%) untypical for garnets from such quartzo-feldspathic rocks

THE VEIN

Though the internal structure of the crosscutting Mn vein is very irregular, an overall zonation can be discerned (Fig. 1b): The borders are rather diffuse and are characterized by greenish garnet which is no longer present in the schist. Then follows a pink rhodonite-zone which irregularly replaces the alabandite core. The vein consists of a sulfide-silicate-carbonate assemblage giving evidence of several generations of mineral growth. While the primary sulfide ore is only preserved in

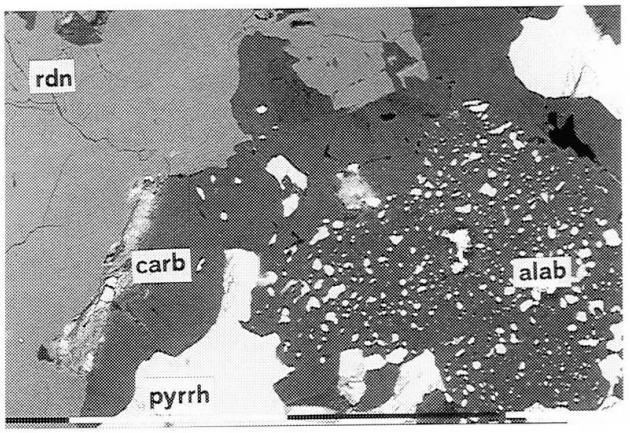

Fig. 2a Backscattered electron micrograph. Rhodonite (rdn; gray) and carbonate (carb; black) formed by replacement of sulfides. Small drop-like grains in carbonate matrix (carb) are relictic alabandite. Carbonate also includes pyrrhotite (pyrrh; white) unaffected by carbonate. No pyrrhotite inclusions are observed within rhodonite (rdn) due to complete replacement by the silicate. Length of bars: 0.1 mm.

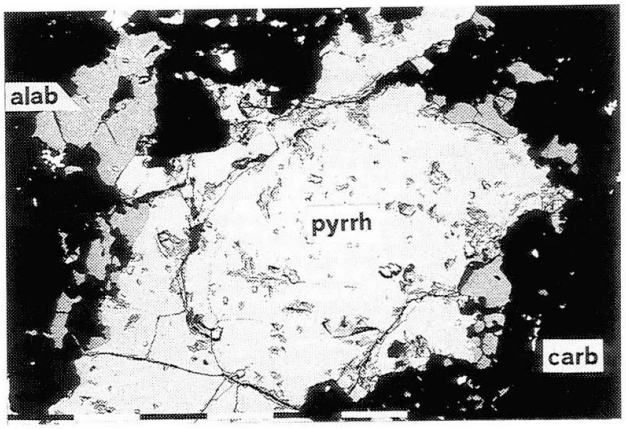

Fig. 2b Backscattered electron micrograph. Relictic alabandite (gray) is strongly replaced by carbonate (carb; black). Large pyrrhotite grain (pyrrh; white) in center is not affected by replacement. Length of bars: 0.1 mm.

Tab. 1 Microprobe analyses of biotites and chlorite

Sample	AM 210-3	AM 210-3	AM 210-2	AM 210-3
Analysis	6-54	7-59	43-90	6-49
Mineral	brown biotite	altered biotite	chlorite	chlorite
SiO_2	38.33	31.96	27.07	26.41
TiO_2	0.42	0.30	0.00	0.09
Al_2O_3	16.83	18.03	20.47	20.37
FeO(1)	12.90	14.97	17.02	17.27
MnO	0.98	1.50	1.87	1.83
MgO	15.25	18.02	20.52	20.02
CaO	0.11	0.00	0.04	0.04
Na_2O	0.04	0.01	0.00	0.00
K_2O	10.36	4.76	0.00	0.00
Sum	95.22	89.55	87.02	86.03
Si	5.692	5.024	5.542	5.484
Al^{IV}	2.308	2.976	2.458	2.502
Ti	0.047	0.035	0.000	0.014
Al^{VI}	0.638	0.365	2.481	2.484
Fe^{2+}	1.602	1.968	2.913	2.999
Mn	0.123	0.200	0.324	0.322
Mg	3.375	4.222	6.261	6.196
Ca	0.017	0.000	0.009	0.009
Na	0.012	0.003	0.000	0.000
K	1.962	0.955	0.000	0.000
Σ(VI)	5.785	----	11.988	12.001

- Biotite formula normalized on an anhydrous basis of 22 oxygens
- Chlorite formula normalized on an anhydrous basis of 28 oxygens

(1) All Fe as FeO

Tab. 2 Mean of microprobe analyses of alabandite and pyrrhotite from AM 210 samples

Mineral	Pyrrhotite	Alabandite
Number of analyses	24	11
Mol% FeS	1.00	0.11
Mol% MnS	<0.001	0.89
Fe p.f.u.	0.467	0.055
Mn p.f.u.	0.001	0.446
S p.f.u.	0.532	0.499

(1) All Fe as FeO

the core, the outer parts of the vein typically display silicate-carbonate parageneses formed by interaction of the sulfide with the host rock.

THE SULFIDES

The internal parts of the vein consist of a mixture of alabandite (MnS) and pyrrhotite (FeS) in variable proportions but with dominant alabandite. Chalcopyrite was found in traces. JENNY (1973) described the two-sulfide assemblage as secondary, formed from a primary Fe-rich alabandite solid solution. Both sulfides show homogeneous compositions (Table 2) indicative of an equilibrium condition for this assemblage. The pyrrhotite is monoclinic (ferromagnetic!) and has a Fe:S ratio close to 7:8, with a MnS content below 0.01 wt%. The coexisting alabandite has the composition $Mn_{0.89}Fe_{0.11}S$ (Table 2). Using the FeS-MnS phase diagram of SUGAKI and KITAKAZE (1972) the coexisting alab-pyrrh pair indicates an equilibrium temperature of about 300°C.

THE SULFIDE-MN SILICATE AND SULFIDE-CARBONATE ASSEMBLAGES

The macroscopic as well as the microscopic features strongly suggest a replacement of the sulfides by rhodonite and/or coarse-grained manganoan calcite (Fig. 2). Rhodonite forms xenomorphic pigmented masses or, less frequently, prismatic grains. The carbonate occurs in cracks within or along the sulfide masses or as inclusions within the massive rhodonite, usually together with pyrrhotite grains. This is in contrast to the more abundant rhodonite which only rarely contains pyrrhotite inclusions. This texture implies that pyrrhotite is replaced by rhodonite, but not by the calcite. Based on these reaction textures and on the contrast in composition between the virtually Fe-free calcite and the Fe-bearing rhodonites (Fig. 3a), the two following desulfidation reactions are proposed:

$$\underset{\text{sulfides}}{FeS} + MnS + \underset{\text{cations in solution}}{Si^{4+} + Ca^{2+} + Mg^{2+}} + 1.5O_2 = \underset{\text{rhodonite}}{(Mn,Ca,Fe,Mg)SiO_3} + S_2 \quad (A)$$

and

$$MnS + Ca^{2+} + CO_2 + 0.5O_2 = (Ca,Mn)CO_3 + 0.5S_2 \quad (B)$$

Similarly, Fig. 2b demonstrates that calcite replaces only the alabandite while the pyrrhotite is hardly affected by the replacement. The calcite formation may be due either to the absence of SiO_2 or locally higher X_{CO_2}. The first possibility is considered more plausible for the rhodonite-garnet veins (Fig. 1c) which do not contain coarse-grained carbonate but abundant quartz. In these veins carbonate did not form due to the presence of sufficient Si^{4+} favoring the formation of the silicate at the given f_{CO_2}. Fine-grained carbonate also occurs as a secondary product formed by retrograde alteration of rhodonite, amphiboles and garnets.

Another striking feature of the veins is the hydration of rhodonite with Mn-bearing amphiboles as products (see below). Chemically, the rhodonites (Table 3) can largely be grouped into low-Ca rhodonites (i) and high-Ca rhodonites (ii):

i) $0.07 < X_{Ca} < 0.14$; typical for rhodonites in alab+pyrrh+spessartine(spess)-rich garnet+carbonate(carb) assemblages

ii) $0.16 < X_{Ca} < 0.22$; in assemblages with grossular-rich garnet+carb.

A clear bimodal distribution is also shown by the garnets (Fig. 3a). Grains from sulfide-bearing assemblages (core of vein) are high in Mn and have grossular components usually below 15 mol%, while garnets formed along the rim of the veins have grossular contents in the range 20-35 mol% (Table 3). The compositional gap between the two groups indicates a two stage formation of the garnets. The Mn-rich group is usually represented by xenomorphic garnets arranged in vein-like strings which are deformed. The Ca-rich garnets are small idiomorphic grains and most likely make part of the (Alpine?) greenschist-facies assemblage biotite(bio) + chlorite(chl) + muscovite(musc) + quartz(qtz) + epidote + sphene in the host rock. The distribution of Mn and Ca between rhodonite und garnet indicates equilibrium between these phases (Fig. 3b). The same behavior in the Ca-Mn distribution is also observed in the carbonates. They have uniformly low Fe- and Mg-contents (< 2 mol%) with

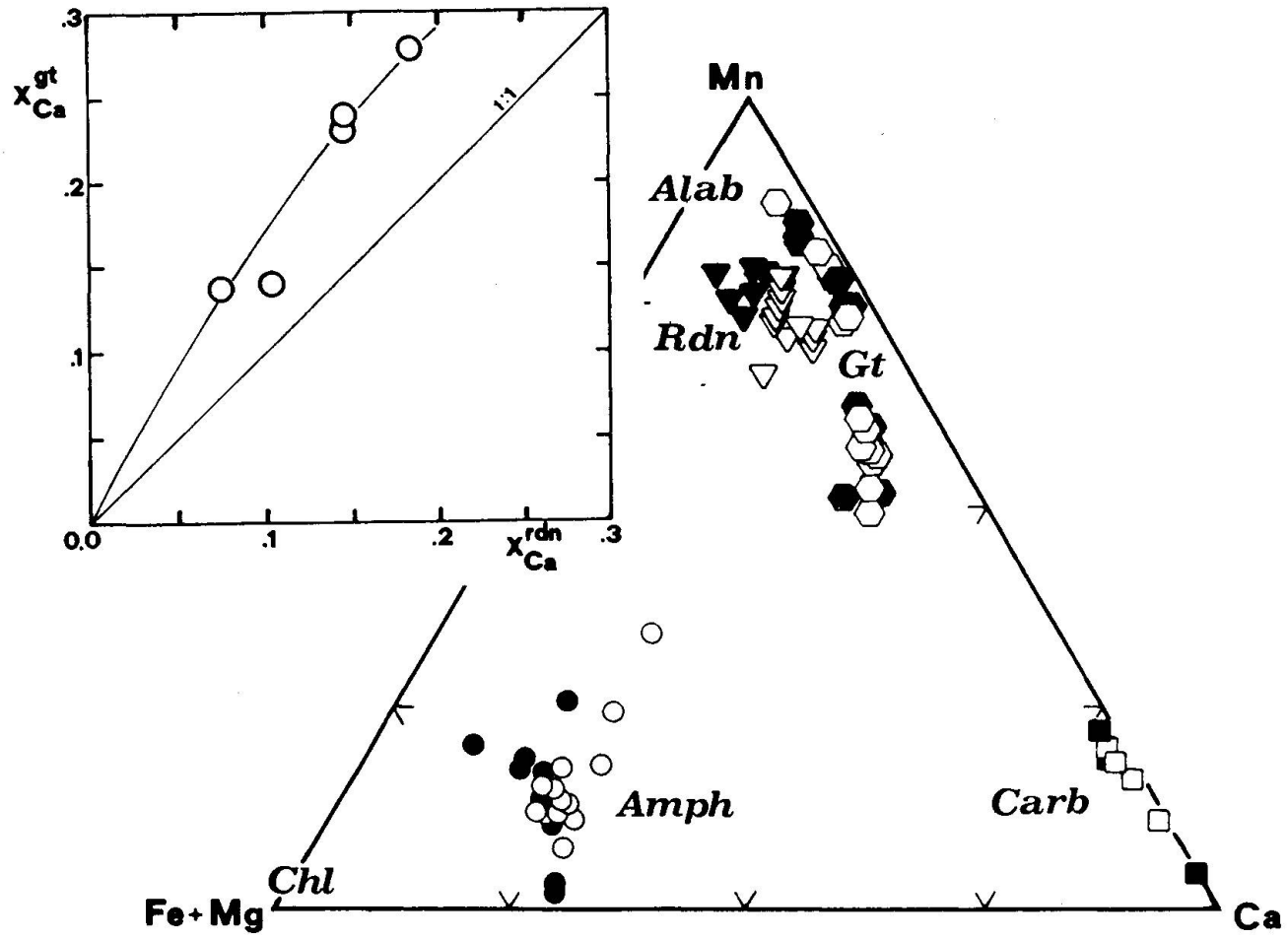

Fig. 3a Fe+Mg - Mn - Ca plot of analyses of samples AM 210-2 (filled symbols) and AM 210-3 (white symbols). A: alabandite; Chl: chlorites from adjoining host rock.
Fig. 3b Distribution of Ca between rhodonites and garnets from sample AM 210-2. Only data from grains in mutual contact are plotted. X_{CA} = Ca/Ca+Mn+Mg+Fe.

rhodochrosite components between 11 and 22 mol%. The coexistence of calcic rhodonite with Ca-rich carbonate is not unusual in manganiferous rocks and the scatter of X_{Rhc} may be due to changing temperature and/or changing X_{CO_2} (ABRECHT, 1985, Fig. 8).

While rhodonite, garnet and carbonate reflect both the zoning of the vein and the existence of local equilibrium, the amphiboles display a more irregular compositional (Table 4) and textural pattern. The amphiboles appear to be the last phase and certainly are not part of the rhodonite-Mn calcite(±Mn-rich spessartine) equilibrium assemblage. They occur in three forms: (a) as epitaxial replacement of rhodonite (see also LIVI and VEBLEN, 1987); (b) as single prismatic grains, sometimes idiomorphic, in the garnet-musc-alkali feldspar(kfsp)-calcite-chl±qtz assemblage; (c) as grains replacing alabandite. Names attributed to the amphiboles in Table 4 are based upon the formulas calculated with a normalization program coded by ROCK and LEAKE (1983). They cover the field of manganoan actinolites (group b and c) to calcic tirodites (group a). Na_2O and K_2O are present only as traces and Al_2O_3 contents vary between 0 and 2 wt%.

Conditions of formation

Former workers (HUTTENLOCHER, 1936; JENNY, 1973) have suggested that the origin of the manganiferous deposit is related to the Variscan magmatism. This view is supported by SCHENKER (1986), although based on different grounds: He relates the sulfide deposits to hydrothermal activities either in connection with the upper-Paleozoic calc-alkaline volcanism or with the subsequent emplacement of the Carboniferous Aar granite. The restriction of the deposits to the tuffaceous members of the volcano-sedimentary series is due to

Tab. 3 Microprobe analyses of garnets and rhodonites

Sample	AM 210-2	AM 210-3	AM 210-2	AM 210-3
Analysis	35-7	2-15	36-13	4-30
Mineral	Garnet	Garnet	Rhodonite	Rhodonite
SiO_2	36.86	37.29	47.18	46.88
TiO_2	0.00	0.26	0.06	0.00
Al_2O_3	21.07	20.91	0.00	0.19
FeO(1)	1.26	0.96	2.17	3.21
MnO	36.29	26.02	44.07	39.81
MgO	0.14	0.25	1.55	0.44
CaO	4.87	12.17	5.52	9.25
Sum	100.49	100.09	100.55	99.89
Si	2.970	2.971	0.998	0.997
Ti	0.000	0.016	0.001	0.000
Al	2.001	1.964	0.000	0.005
Fe^{2+}	0.085	0.213	0.038	0.057
Mn	2.477	1.765	0.790	0.717
Mg	0.017	0.030	0.049	0.014
Ca	0.420	1.039	0.125	0.211
X_{Mn}	0.83	0.59	0.79	0.72
X_{Ca}	0.11	0.31	0.12	0.21
a_{MnSiO3}			0.77	0.66

- Garnet formulas calculated on a basis of 5 cations
- Rhodonite formulas calculated on a basis of 3 oxygens

(1) All Fe as FeO

Tab. 4 Microprobe analyses of amphiboles

Sample	AM 210-3	AM 210-3	AM 210-2	AM 210-2
Analysis	2-19	8-62	10-79	35-8
Mineral(1)	actinolite	manganoan actinolite	manganese tremolite	tirodite
SiO_2	55.00	55.59	56.09	54.64
TiO_2	0.00	0.06	0.00	0.00
Al_2O_3	1.82	0.47	0.23	0.00
FeO(2)	6.70	6.05	2.35	5.64
MnO	1.96	3.87	8.40	9.92
MgO	18.30	17.70	19.09	17.77
CaO	12.59	12.26	10.23	7.90
Na_2O	0.26	0.07	0.07	0.01
K_2O	0.02	0.00	0.00	0.00
Sum	96.65	96.07	96.46	95.88
Si	7.797	7.948	7.956	7.977
Ti	0.000	0.006	0.000	0.000
Al	0.304	0.079	0.038	0.000
Fe^{3+}(3)	0.202	0.236	0.279	0.047
Fe^{2+}(3)	0.592	0.487	0.000	0.642
Mn	0.236	0.469	1.010	1.228
Mg	3.869	3.774	4.038	3.869
Ca	1.912	1.878	1.555	1.236
Na	0.071	0.019	0.019	0.003
K	0.004	0.000	0.000	0.000

(1) Amphibole names according to IMA nomenclature ROCK and LEAKE (1983)

(2) All Fe as FeO

(3) Ferric and ferrous iron calculated according to normalization scheme by ROCK and LEAKE (1983) on an anhydrous basis of 23 oxygens

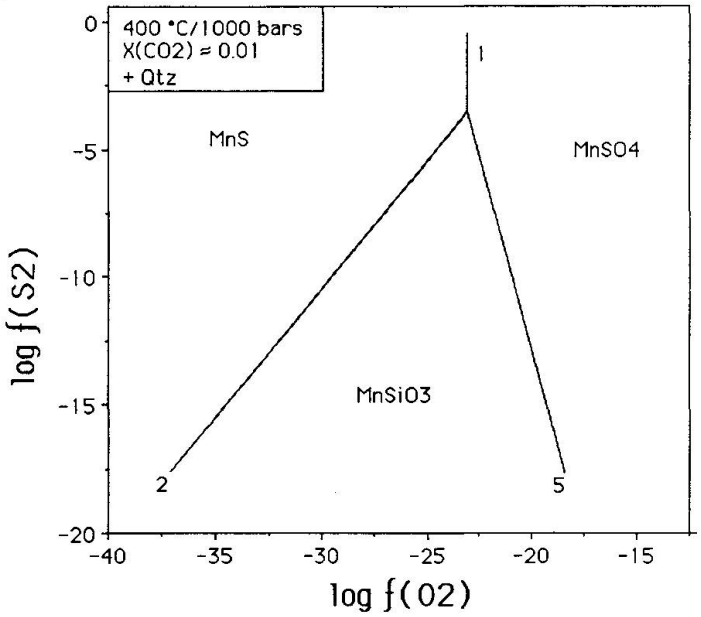

Fig. 4a log fs_2 vs. log fo_2 diagram for the system Mn-O-S at 400°C/1 kbar for pure phases (excess SiO_2 present).

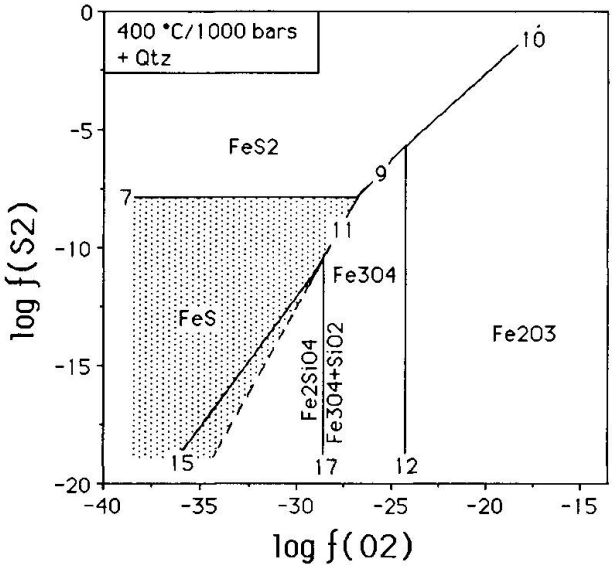

Fig. 4b log fs_2 vs. log fo_2 diagram for the system Fe-O-S at 400°C/1 kbar for pure phases (excess SiO_2 present). The dotted field represents the pyrrhotite stability field in the absence of quartz.

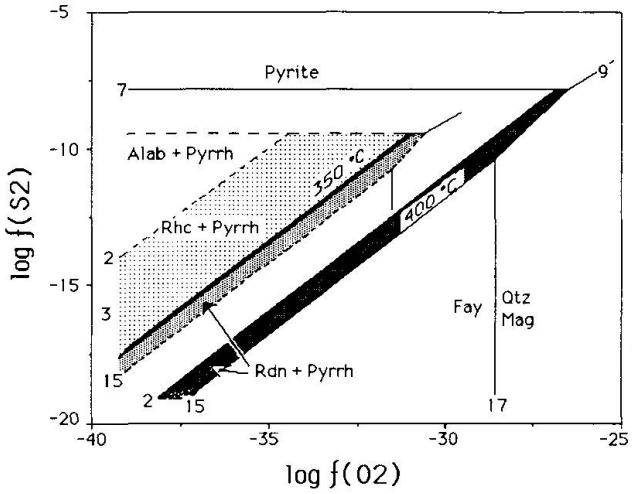

Fig. 4c log fs_2 vs. log fo_2 diagram for possible vein-forming conditions (400°C/1 kbar) and lower greenschist-facies conditions (350°C/3 kbar). Thick lines represent reaction (3) for equilibrium mole fractions of CO_2 (numbers in brackets) as calculated from data in ABRECHT (1988) for the given P-T conditions. Dark shaded areas represent the stability fields for rhodonite + pyrrhotite at both given temperatures. Light shaded area represents the Mn calcite+pyrrhotite stability field at 350°C/3 kbar for X_{CO_2} 0.01.
Curves are drawn for activities as given in the Appendix. Thermochemical data from HELGESON et al. (1979) and ABRECHT (1988). Numbers refer to numbers of reactions given in Table 5.

their higher permeability for meteoric water and hydrothermal solutions. Except the alabandite deposits, the sulfide deposits are probably impregnations of the host rock (pyrite-bearing sericite-schists of JENNY, 1973) with the development of vein-like features (Fig. 1a). This may indeed indicate high porosity and thus increased permeability with respect to ore-forming solutions and points to an epithermal origin related to upper-Paleozoic volcanic activity. The sometimes intense alteration of potassic feldspar to muscovite (sericite) described by most authors and also observed in the samples studied here, was interpreted by SCHENKER (1986) as a product of this activity. In fact, he considers the biotite-sericite gneisses, the pyrite-rich sericite-schists, and the chlorite-sericite-schists as an alteration sequence produced by hydrothermal processes in geothermally active, silicic volcanic terranes (typically around porphyry coppers or epithermal ore deposits; see for example ROSE and BURT, 1979). Thus, the present lithologies may represent a former sequence from propylitic to sericitic alteration zones, later metamorphosed under greenschist facies conditions. Because the Mn ore occurs in a slightly different mode, (viz. as distinct veins clearly crosscutting the host rock structures, Fig. 1a) it may belong to another stage of ore formation. Possibly, this is related to the emplacement of the Aar granite. JENNY (1973) has suggested the exsolution of a primary single-phase Mn-Fe sulfide, leading to a mixture of predominant Fe-bearing alabandite and minor pyrrhotite. Based upon the estimated amount of the present pyrrhotite (about 5 vol%) a primary bulk sulfide composition of $Mn_{.85}Fe_{.15}S$ can be calculated. For a homogeneous Mn-Fe sulfide with this composition the phase diagram by SUGAKI and KITAKAZE (1972) indicates a minimum exsolution temperature of around

Tab. 5 Reactions in the system Mn–Si–O–C–S and Fe–O–S used for the calculations of diagrams (Figures 4 and 5)

$MnS + 2O_2$	$= MnSO_4$	[1]
$MnS + SiO_2 + 0.5O_2$	$= MnSiO_3 + 0.5S_2$	[2]
$MnS + CO_2 + 0.5O_2$	$= MnCO_3 + 0.5S_2$	[3]
$MnCO_3 + 0.5S_2 + 1.5O_2$	$= MnSO_4 + CO_2$	[5]
$MnSiO_3 + 0.5S_2 + 1.5O_2$	$= MnSO_4 + SiO_2$	[6]
$FeS + 0.5S_2$	$= FeS_2$	[7]
$2FeS_2 + 1.5O_2$	$= Fe_2O_3 + 2S_2$	[8]
$3FeS_2 + 2O_2$	$= Fe_3O_4 + 3S_2$	[9]
$2FeS + 1.5O_2$	$= Fe_2O_3 + S_2$	[10]
$3FeS + 2O_2$	$= Fe_3O_4 + 1.5S_2$	[11]
$2Fe_3O_4 + 0.5O_2$	$= 3Fe_2O_3$	[12]
$2FeS + SiO_2 + O_2$	$= Fe_2SiO_4 + S_2$	[15]
$2Fe_3O_4 + 3SiO_2$	$= 3Fe_2SiO_4 + O_2$	[17]

400°C. Re-equilibration during further cooling produced the present composition of the coexisting sulfide phases.

Whether monoclinic pyrrhotite is a stable phase or not is still a matter of debate. Nevertheless, its occurrence with the composition Fe_7S_8 (≈ 46.6 atom% Fe) is most likely due to low temperature recrystallization of an originally hexagonal pyrrhotite phase (BARTON and SKINNER, 1979). According to the same authors, pyrrhotite having this composition would only be stable at T > 500°C, indicating a high-temperature formation. However, low-T re-equilibration at different fs_2 may have changed the Fe:S ratio.

The formation of the manganiferous silicates (rhodonite, ±garnet) may well be related to the hydrothermal alteration of the parent rock. Solutions in equilibrium with the silicic host rock supplied the required material for the silicate formation within the vein. Certainly, sufficient silica could be provided by hydrolysis of potassic feldspar, and calcium, aluminum and magnesium were simultaneously transferred to the vein (ROSE and BURT, 1979). The Mn-bearing actinolite (type b) and most of the Ca-rich garnet are probably products of the Alpine metamorphism. These phases formed after the folding of the vein (Fig. 1c) attributed to Alpine deformation.

Figure 5 shows the evolution scheme for the vein. It is suggested that the present veins are derivatives of primary hydrothermal (single phase?) sulfide veins (Stage I and II) which were desulfidized due to infiltration of hydrothermal solutions enriched in silicon, calcium, aluminum and magnesium at moderate temperatures (Stage III). Only the present sulfide composition as well as the Ca-rich garnets and amphiboles are products of the Tertiary greenschist-facies metamorphism (Stage IV).

Provided the temperature-pressure conditions during the different stages of mineral formations are given, the observed phase assemblages can be used for an estimation of the vapour composition (fo_2, fs_2, fCO_2). Based on the given evolution model a temperature of 400°C at 1 kbar pressure was assumed for stage III, while for the greenschist metamorphism 350°C/3 kbar were assumed (the effect of the pressure on the following calculations is negligible). In a fo_2-fs_2 space the alabandite has a rather restricted stability (GARRELS and CHRIST, 1965). The reactions given in Table 5 constrain the stability of some mineral phases relevant to the manganiferous rock considered here. Because of the uncertainty in the P-T conditions and the too many unknowns we cannot unequivocally determine the fluid fugacities. However, some limiting values for fo_2, fs_2 and fCO_2 can be derived from appropriate diagrams (Fig. 4). Figure 4 is constructed for rhodonite, carbonate, and alabandite compositions observed in the present samples (see Tables 1 and 2). For the thermodynamic calculations mixing models had to be used, which are described shortly in Appendix. The $logfs_2$-$logfo_2$ diagrams in Fig. 4a and 4b give the topology of the Fe-O-S(+SiO_2) and the Mn-O-S (+ SiO_2) systems at 400°C/1 kbar for pure phases. In Fig. 4c only

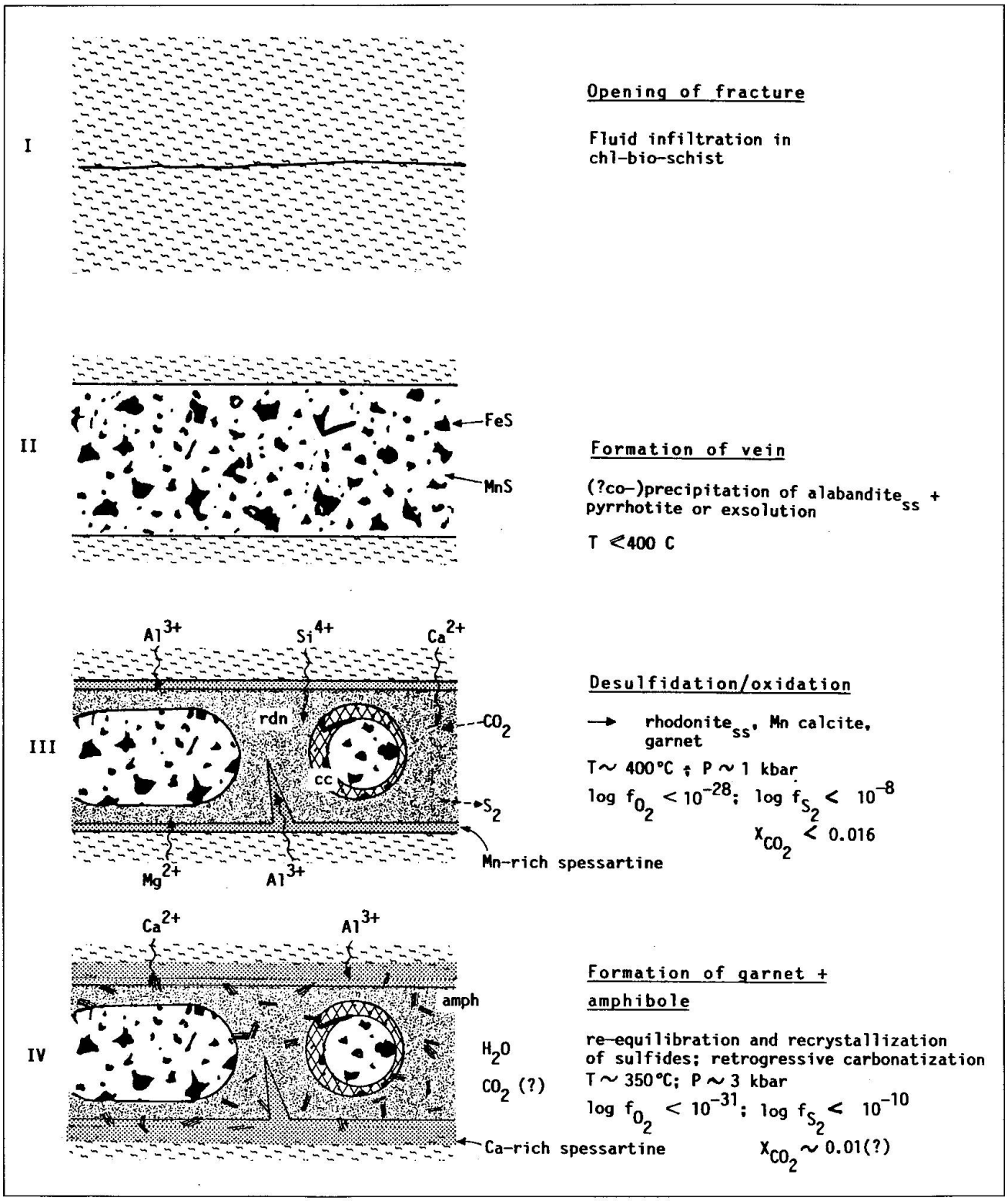

Fig. 5 Stages of vein formation and alteration. See text for explanations.

reactions relevant to the manganiferous rock are considered and the solid solution nature of the phases is taken into account. Quartz is present as an excess phase.

The presence of stable Mn calcite indicates that CO_2 was present. The appearance of CO_2 yields further reactions involving carbonate, such as reaction (3) (represented by a hatched line). As discussed before, the growth of carbonate may be due to lacking Si^{4+}-supply, but also to locally increased fCO_2 or decreasing temperatures. The alabandite-Mn carbonate univariant curve (reaction 3) is given

only for 350°C/3 kbar. The curve was drawn for $X_{CO_2} \approx 0.01$. Using new thermochemical data for rhodonite (ABRECHT, 1988), the reaction $MnCO_3 + SiO_2 = MnSiO_3 + CO_2$ was used to calculate the maximum X_{CO_2} for rhodonite ($X_{Mn} = 0.79$) being a stable phase with respect to Mn calcite. The obtained values ($X_{CO_2} = 0.016$ at 400°C/1 kbar; $X_{CO_2} = 0.0004$ at 350°C/3 kbar) were used for the construction of the reaction (2) (thick curves). Reactions (2), (11) and (15) delineate the rhodonite+pyrrhotite stability field (dark stippled areas) while Mn-calcite+pyrrhotite are stable within the light stippled area at greenschist facies conditions. It becomes obvious that the assemblage pyrrhotite + rhodonite has a rather limited stability field in fO_2-fS_2 space ($fO_2 < 10^{-28}$ at 400°C/1 kbar and fS_2 below 10^{-8}). This narrow field is shifted to even lower values at 350°C/3 kbar. The maximum oxygen fugacities for these assemblages are in the range of fugacities defined by the quartz-magnetite-fayalite buffer (17). The resulting fugacities are not sensitive to changes in pressure and differ by about two long units for the two temperature/pressure conditions.

Origin of the alabandite-silicate assemblage: Discussion and summary

With the available material and data little can be said about the mode of formation of the Mn sulfide. Alabandite seems to form generally as a vein-type mineral (FUKUOKA, 1981; HEWITT and ROVE, 1930). Its replacement by carbonate and silicate has been described from other localities (see HEWETT and ROVE , 1930) but was not examined in detail. The observed mode of occurrence in the Amsteg water tunnel also indicates a vein-type deposit within tuffaceous volcanic rocks infiltrated by Mn-bearing hydrothermal solutions. Manganese is one of the metals that are strongly concentrated in the aqueous phase derived from acid magmas (HOLLAND, 1972). Experimental data by BOCTOR (1985) indicate that in Cl-bearing solutions Mn is complexed as $MnCl_2$. Its deposition may then be monitored by a reaction such as

$$MnCl_2 + H_2S = MnS + 2H^+ + 2Cl^- \qquad (C)$$

Reaction (C) shows that, apart from falling temperatures, MnS deposition may be caused by increase in pH, addition of H_2S or dilution of the aqueous phase. In a shallow environment as envisaged for the Amsteg deposit, dilution by meteoric waters may in fact play a role. Such mixing could ultimately be one of the reasons for the rhodonite growth which is favoured by decreasing sulfur activity (Fig. 4). The sulfide veins were altered by ore-fluid interaction and later low-grade metamorphism. The required ions (Si^{4+}, Ca^{2+}, Al^{3+}, Mg^{2+}, OH^-) were supplied by water-rich fluids infiltrating the quartzo-feldspathic host rock, leading to rhodonite-garnet-carbonate assemblages. At lower temperatures, probably during the Alpine greenschist metamorphism, hydration of rhodonite (and to a lesser extent of alabandite) caused the formation of Mn-bearing amphiboles and calcic garnets. Dissolution and recrystallization of minerals involving manganese (during Alpine metamorphism?) is indicated by the increased MnO-content of host-rock chlorites formed from biotites primarily low in Mn.

Acknowledgments

The paper greatly benefited from the (very) critical comments by Franz Schenker and Urs Raz. I would like to thank Mark Handy for correcting the English and Jim Craig and Lukas Baumgartner for discussions. The Labor für Rasterelektronenmikroskopie der Universität Basel generously provided help and facilities. Hans Schwander assisted in microprobe analysis.

References

ABRECHT, J. (1985): Manganiferous pyroxenes and pyroxenoids from three Pb-Zn-Cu skarn deposits. Contrib. Mineral. Petrol. 89, 379-393.

ABRECHT, J. (1988): Experimental evaluation of the $MnCO_3 + SiO_2 = MnSiO_3 + CO_2$ equilibrium at 1 kbar. American Mineral. 73, 1285-1291.

BARTON, JR., P. B. and SKINNER, B. J. (1979): Sulfide mineral stabilities. In: Geochemistry of hydrothermal ore deposits. (ed.) Barnes, H. L.. John Wiley & Sons, New York, 278-403.

BOCTOR, N. Z. (1985): Rhodonite solubility and thermodynamic properties of aqueous $MnCl_2$ in the system MnO-SiO_2-HCl-H_2O. Geochim. Cosmochim. Acta 49, 565-575.

CAPITANI, C., DE, and PETERS, T. (1981): The solvus in the system $MnCO_3$-$CaCO_3$. Contrib. Mineral. Petrol. 76, 394-400.

DAVIES, P. K. and NAVROTSKY, A. (1983): Quantitave correlations of deviations from ideality in binary and pseudo-binary solid solutions. J. Solid State Chem. 46, 1-22.

FREY, M., BUCHER, K., FRANK, E. and MULLIS, J. (1980): Alpine metamorphism along the geotraverse Basel–Chiasso - a review. Eclogae geol. Helv. 73, 527-546.

FUKUOKA, M. (1981): Mineralogical and genetical study on alabandite from the manganese deposits of Japan. Mem. fac. Sci., Kyushu Univ., Ser. D. Geol., XXIV, No. 4, 207-251.

FUKUOKA, M. and HIROWATARI, F. (1977): Alabandite in the bedded ore deposits in the Seta districts, Gumma Prefecture. Mining Geol. 27, 401-414.

GARRELS, R. M. and CHRIST, C. L. (1965): Solutions, minerals and equilibria. Freeman, Cooper and Co., San Francisco.

HELGESON, H. C., DELANY, J. M., NESBITT, H. W. and BIRD, D. K. (1978): Summary and critique of the

thermodynamic properties of rock-forming minerals. American J. Sci. 278-A, 1-229.
HEWETT, D. F. and ROVE, O. N. (1930): Occurrence and relations of alabandite. Econ. Geol. 25, 36-56.
HOLLAND, H. D. (1972): Granites, solutions and base metal deposits. Econ. Geology 67, 281-301.
HUGI, E. (1921a): Pneumatolytisch-hydrothermale Wirkungen alpiner Granitintrusionen. Eclogae geol. Helv. 16, 464-482.
HUGI, E. (1921b): Original notes and sketches from the water tunnel.
HUGI, E. (1923): Über einige Gesteins- und Mineralvorkommnisse der Wasserstollen des Kraftwerkes Amsteg (Uri). Schweiz. mineralog. petrogr. Mitt. 3, 263-297.
HUTTENLOCHER, H. (1936): Zur Mangan-Zinn-Silber-Lagerstätte aus dem Wasserstollen des Amsteger Kraftwerkes. Schweiz. mineralog. petrogr. Mitt. 16, 406-408.
JENNY, J.-P. (1973): Die Vorkommen von Bleiglanz, Kupferkies und Zinkblende des Bristenstocks (Kt. Uri). Beitr. Geol. Schweiz, Geotechn. Ser., Lfg. 53.
LIVI, K. J. T. and VEBLEN, D. R. (1987): Analytical electron microscopy (AEM) of a pyroxene-to-pyroxenoid reaction. Abstr. AGU Spring Meet. 1987, EOS 68, 453.
OBERHÄNSLI, R., SCHENKER, F. and MERCOLLI, I. (1988): Indications of Variscan nappe tectonics in the Aar massif. Schweiz. mineralog. petrogr. Mitt. 68, 507-518.
PFLUGSHAUPT, P. (1927): Beiträge zur Petrographie des östlichen Aarmassivs. Schweiz. mineralog. petrogr. Mitt. 7, 321-378.
ROCK, N. M. S. and LEAKE, B. E. (1984): The international Mineralogical Association amphibole nomenclature scheme: computerization and its consequences. Miner. Mag. 48, 211-227.
ROSE, A. W. and BURT, D. M. (1979): Hydrothermal alteration. In: Geochemistry of hydrothermal ore deposits. (ed.) Barnes, H. L.. John Wiley & Sons, New York, 173-235.
ROY, S. (1981) Manganese deposits. Academic Press, London.
SCHALTEGGER, U. (1986): Geochemie und Rb-Sr-Systematik der Aarmassiv-Granite zwischen Grimsel und Reusstal. Schweiz. mineralog. petrogr. Mitt. 66, 462-466.
SCHENKER, F. (1986): Spätpaläozoischer saurer Magmatismus und Beckenbildung im Aarmassiv unter kompressiver Tektonik. Unpubl. PhD thesis, Bern.
SCHENKER, F. (1987): Hinweise für kompressive Tektonik während der Ablagerung von oberpaläozoischen Sedimenten und Vulkaniten im Aarmassiv. Bull. Ver. schweiz. Petroleum-Geol. u. Ing., 54, 45-57.
SCHENKER, F. and ABRECHT, J. (1987): Prä-aargranitische Anatexis, variszische Kontaktmetamorphose und alpidische Regionalmetamorphose im Oberhasli (Zentrales Aarmassiv, Schweiz). Schweiz. mineralog. petrogr. Mitt. 67, 1-13.
SUGAKI, A. and KITAKAZE, A. (1972): In: FUKUOKA, M. and HIROWATARI, F. (1977).

Manuscript received November 11, 1988; revised manuscript accepted February 17, 1989.

Appendix

For rhodonite, carbonate and alabandite the following mixing models were applied for the calculation of the activities.

Carbonate: Mainly a $MnCO_3$-$CaCO_3$ solid solution. The Margules parameters derived from the experimentally determined binary solvus (CAPITANI, DE and PETERS, 1981) were used for the calculation of $MnCO_3$ activity in the carbonate phase.

Rhodonite: A quaternary solution of (Mn-Ca-Fe-Mg)SiO_3. No experimental data on mixing properties are available. A modified version (ABRECHT, 1985) of the "on-site mixing" model by WINTER et al. (1980) was applied to calculate $MnSiO_3$ activity in rhodonite.

Alabandite: A MnS-FeS solid solution. The experimentally determined miscibility gap between pyrrhotite and alabandite (SUGAKI and KITAKAZE, 1972) was used for the derivation of interaction parameters. Because original experimental data were not available, the T-X_{Mn} diagram (Figure 1 in FUKUOKA and HIROWATARI, 1977) was taken for this purpose. A two-parameter subregular mixing model (e. g. DAVIES and NAVROTSKY, 1983) was applied. The W_{G1}- and W_{G2}-parameters were calculated according to equations (20) and (21) from DAVIES and NAVROTSKY (1983) and then fitted against the temperature with a second-order polynomial which yielded

$$W_{G1} = 13860 - 23.37T + 0.0337T^2$$
$$W_{G2} = 7815 + 62.79T - 0.0491T^2$$

The following compositions and activities for the solid solution minerals were used for the construction of Fig. 4:

Carbonate: X_{MnCO_3}	= 0.20	a_{MnCO_3}	= 0.39
Rhodonite: X_{MnSiO_3}	= 0.79	a_{MnSiO_3}	= 0.77
Alabandite: X_{MnS}	= 0.89	a_{MnS}	= 0.90